PROPAGATION OF MICROWAVES ON A SINGLE WIRE—PART II

BY S. N. CONTRACTOR AND S. K. CHATTERJEE

(*Department of Electrical Communication Engineering, Indian Institute of Science, Bangalore-3*)

Received October 19, 1956

ABSTRACT

Expressions for the longitudinal and transverse impedance have been derived from the field components of the E_0 wave with which the surface wave line is excited. Three different types of terminations have been attempted to match the line. The results of v.s.w.r. measurements with probe placed in the E_z and E_r orientations at different radial distances from the surface wave line exhibit the superiority of a tapered wooden termination fixed with cardboard fins sprayed with graphite as a matching device.

FIELD COMPONENTS OF SURFACE WAVE

The surface wave that can be associated with a cylindrical conductor embedded in an isotropic, homogeneous dielectric medium of infinite extent is characterized by the presence of an axial component of the $\vec{E}$ vector and complete absence of the longitudinal component of the $\vec{H}$ vector. The energy density of the electromagnetic field for this wave decreases in the radial direction from the axis of the surface wave line. The rate of decay of energy is determined by the radius of the line and the surface wave impedance. The surface wave impedance is provided by the guided wave inside the line. However, this inside wave contributes very little so far as surface wave phenomena is concerned as the mean axial flow of energy within the guide is zero. The non-zero field components of the axially symmetric E_0 wave with which the surface wave line is excited are outside the line ($r > a$) of radius a.

$$
\begin{aligned}
E_{r2} &= jA \frac{h}{\gamma_2} H_1^{(1)} (\gamma_2 r) e^{-jhz} \\
E_{z2} &= AH_0^{(1)} (\gamma_2 r) e^{-jhz} \qquad (1) \\
H_{\phi 2} &= jA \frac{k_2^2}{\omega \mu_2 \gamma_2} H_1^{(1)} (\gamma_2 r) e^{-jhz}
\end{aligned}
$$

where A is the excitation constant and H's represent the Hankel functions of the first kind. The subscript 2 indicates the region outside the wire.

Surface Impedance

The surface impedance Z_s of the line acting as a guide is defined as

$$Z_s = \left.\frac{E_{z2}}{H_{\phi 2}}\right|_{r=a} \tag{2}$$

where E_{z2} and $H_{\phi 2}$ are the tangential components of $\vec{E}$ and $\vec{H}$ respectively. The impedance is evaluated on the surface of the line. From equations (1) and (2)

$$Z_s = -\frac{j\omega\mu_2\gamma_2}{k_2^2}\,\frac{H_0^{(1)}(\gamma_2 a)}{H_1^{(1)}(\gamma_2 a)} \tag{3}$$

where

$$k_2^2 = \omega^2\mu_2\epsilon_2 = \omega^2\mu_0\epsilon_0$$

$$\gamma_2 = \text{axial propagation constant} = (k_2^2 - h^2)^{1/2}$$

$$h = \text{propagation factor}$$

For $\gamma_2 a \ll 1$, the ratio of the two Hankel functions is (Sommerfeld, 1927)

$$\frac{H_0^{(1)}(\gamma_2 a)}{H_1^{(1)}(\gamma_2 a)} \cong -\gamma_2 a \, ln \frac{j\gamma\,\gamma_2 a}{2} \tag{4}$$

where $\gamma = 1 \cdot 781$.

From (3) and (4) the following expressions for Z_s is obtained

$$Z_s = -\frac{\pi\omega\gamma_2^2\mu_2 a}{2k_2^2} + j\left[\frac{\omega\gamma_2^2\mu_2 a}{k_2^2}\, ln\,\frac{\gamma}{2} + \frac{\omega\gamma_2^2\mu_2 a}{k_2^2}\, ln\,(\gamma_2 a)\right]$$

$$= R_s + jX_s. \tag{5}$$

In order to calculate Z_s from the above expression, γ_2 must be evaluated.

The surface wave for the E_0 mode supported by a cylindrical conductor immersed in air is governed by the following well-known equation (Stratton, 1941)

$$\frac{H_0^{(1)}(\gamma_2 a)}{H_1^{(1)}(\gamma_2 a)} = \frac{k_2^2}{k_1^2}\,\frac{\mu_1\gamma_1}{\mu_2\gamma_2}\,\frac{J_0(\gamma_1 a)}{J_1(\gamma_1 a)} \tag{6}$$

where

$$\gamma_1^2 = k_1^2 - h^2, \quad \gamma_2^2 = k_2^2 - h^2, \quad k_1 = \alpha_1 + j\beta_1.$$

Since $\gamma_1 a \gg 1$ we can replace J_0 and J_1 by their asymptotic expressions and since for large conductivity $\alpha_1 \simeq \beta$ and $\gamma_1 \simeq k_1$, the following expression is obtained from (4) and (6)

$$(\gamma_2 a)^2 \, ln \frac{\gamma\gamma_2 a}{2j} = j\,\frac{k_2^2 a}{k_1}\,\frac{\mu_1}{\mu_2} \tag{7}$$

where

$$\lim_{\beta_1 \to \infty} \frac{J_1(\gamma_1 a)}{J_0(\gamma_1 a)} = -j \tag{8}$$

From (7) the following expression for γ_2 is obtained

$$\left(\frac{\gamma\gamma_2 a}{2j}\right)^2 = -1 \cdot 75 \times 10^{-13} \frac{(1-j)}{20} a\nu \sqrt{\frac{\nu}{\sigma_1}}$$

or

$$\gamma_2 = 1 \cdot 202 \times 10^{-9} (1-j)^{\frac{1}{2}} \nu^{\frac{3}{4}} a^{-\frac{1}{2}} \tag{9}$$

From equations (5) and (9) the following expressions for the real and the imaginary parts of Z_s are obtained.

$$R_s = \frac{\pi\mu_2 \nu^{5/2}}{k_2^2} \left[ln\,(a\nu^{3/2}) - \frac{\pi}{2} - 41 \cdot 313 \right] \times 1 \cdot 445 \times 10^{-18} \tag{10}$$

$$X_s = \frac{\pi\mu_2 \nu^{5/2}}{k_2^2} \left[ln\,(a\nu^{3/2}) + \frac{\pi}{2} - 41 \cdot 313 \right] \times 1 \cdot 445 \times 10^{-18}$$

where $\omega = 2\pi\nu$.

In a similar way, the longitudinal impedance defined as

$$Z_z = \left. \frac{E_{r2}}{H_{\phi 2}} \right|_{r=a} \tag{11}$$

is found from (1) and (11) as follows

$$Z_z = \sqrt{\frac{\mu_2}{\epsilon_2}} \cong \sqrt{\frac{\mu_0}{\epsilon_0}} \tag{12}$$

which is the same as the impedance of the free space. It is obvious that $Z_s \gg Z_z$. Consequently, $E_{r2} \gg E_{z2}$. This enables one to visualise the structure of the field in the vicinity of the surface wave guide. The field lines emerge from the guide almost perpendicular to the surface of the guide with very little forward tilt, provided the conductivity of the surface of the guide is high. The wave, however, proceeds in the dielectric medium along the surface with alternate charges moving in the field. This means that the forward tilt of the wavefront may be used as a measure of the surface conductivity of the guide. Any forward tilt of the wave will cause an angular displacement between the equiphase and the equiamplitude surfaces of the wave. A measure of the angular displacement will lead to an understanding of the inhomogeneity of wave.

MATCHING OF THE SURFACE WAVE LINE

The matching of the surface wave line depends to a certain extent on the type and dimensions of the launching device and also on the distance between the transmitting and the receiving end. The launching device used in the present investigations is a conical horn which may be considered as a field transformer which transforms the field of a conical guide to the field of the surface wave. As the field extends radially to infinity, the matching between the field of the surface wave and the field of the launching device is rather difficult to achieve. The larger the launching device and longer the surface wave line, the chances of achieving perfect matching are greater. The length of the line and the dimensions of the launching device have been restricted in the present case due to practical considerations. No detail study of the matching of a surface wave line of limited length has yet been reported by any previous worker to the best knowledge of the authors. In a recent paper (Chatterjee *et al.*, 1955) an attempt was made to match the surface wave line by means of matching stubs at the transmitting and the receiving ends of the line and also by means of a tapered wooden termination at the receiving end. As a proper matching of the line is essential for the accurate measurement of the radial field spread, it has been considered worthwhile to explore the possibilities of finding a suitable termination for the surface wave line.

EXPERIMENTAL

An experimental study of the matching of the surface wave line ($\lambda = 3\cdot 2$ cm.) involves the measurement of v.s.w.r. at different points of the line. As the values of the radial and longitudinal impedances are different, it is obvious that the v.s.w.r. measured at any distance from the transmitting end will be different at different radial distances from the surface of the conductor. The v.s.w.r. depends on E_{z2} and E_{r2}. These two components have been measured separately by the probe method as described elsewhere (Chatterjee, *loc. cit.*). The orientation of the probe for the measurement of E_z is shown in photograph, Fig. 18 of Part I. The orientation of the probe for the measurement of E_r is shown in Fig. 1. The probes have been placed parallel to E_z and E_r respectively in the two cases.

The matching of the line in addition to having stubs at both the ends has been attempted by three different types of terminations placed at the receiving end of the line as follows:—

(i) Tapered wooden terminations of varying dimensions.

(ii) Different absorbing materials placed inside the receiving horn.

(iii) Tapered wooden termination with cardboard fins deposited with graphite powder.

(i) *Tapered Wooden Terminations.*—In order to match the line, wooden terminations of different dimensions were attempted. The results of the measurement are presented in Table I. A sketch of the termination is shown in Fig. 2.

The variation of v.s.w.r. with radial distances for different terminations is shown in Fig. 3. Some of the results of measurements showing the variation of v.s.w.r. with respect to D/λ, $(L - l)/\lambda$ and α are shown graphically in Figs. 4, 5, and 6

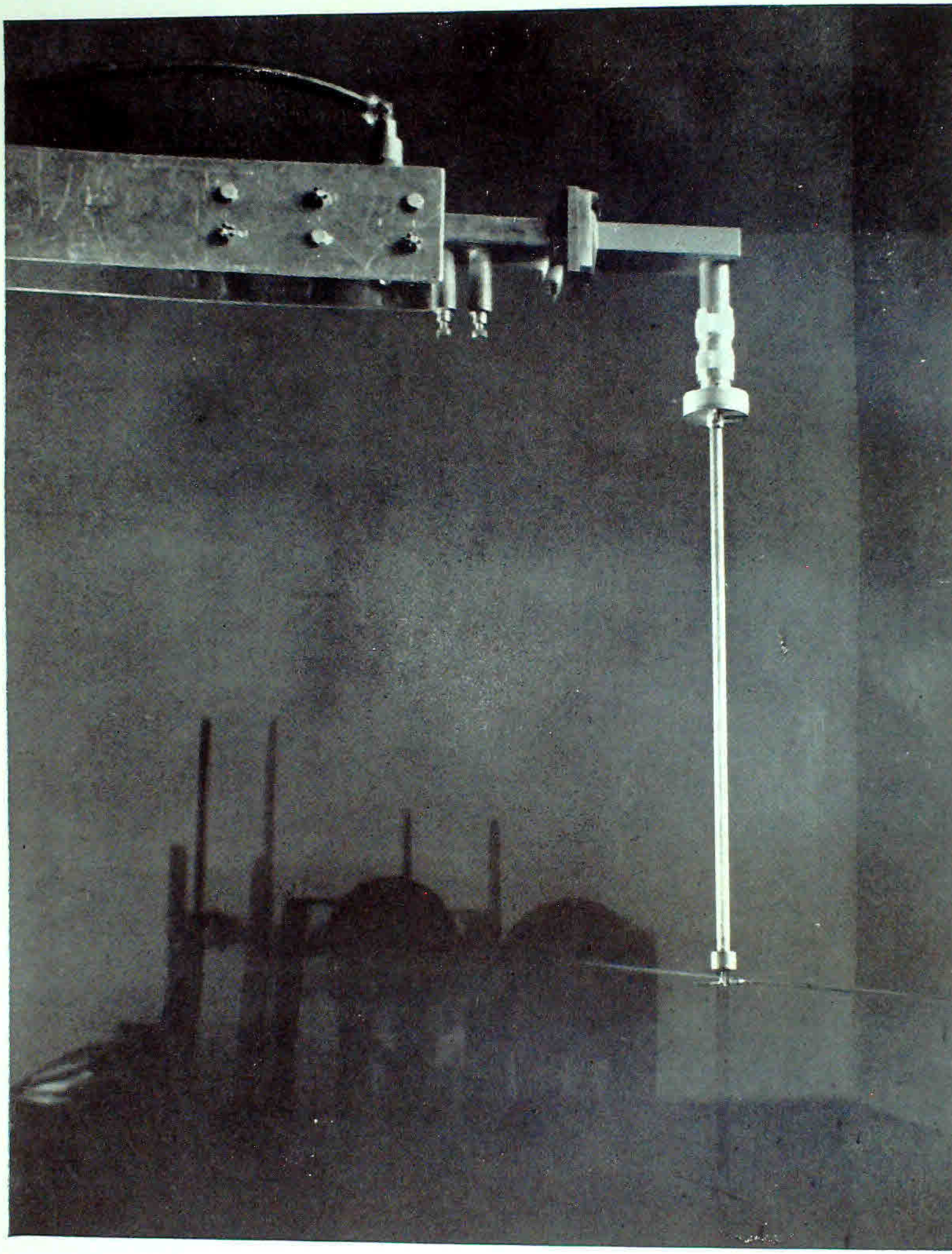

FIG. 1. Photograph of the probe placed in the E_r orientation.

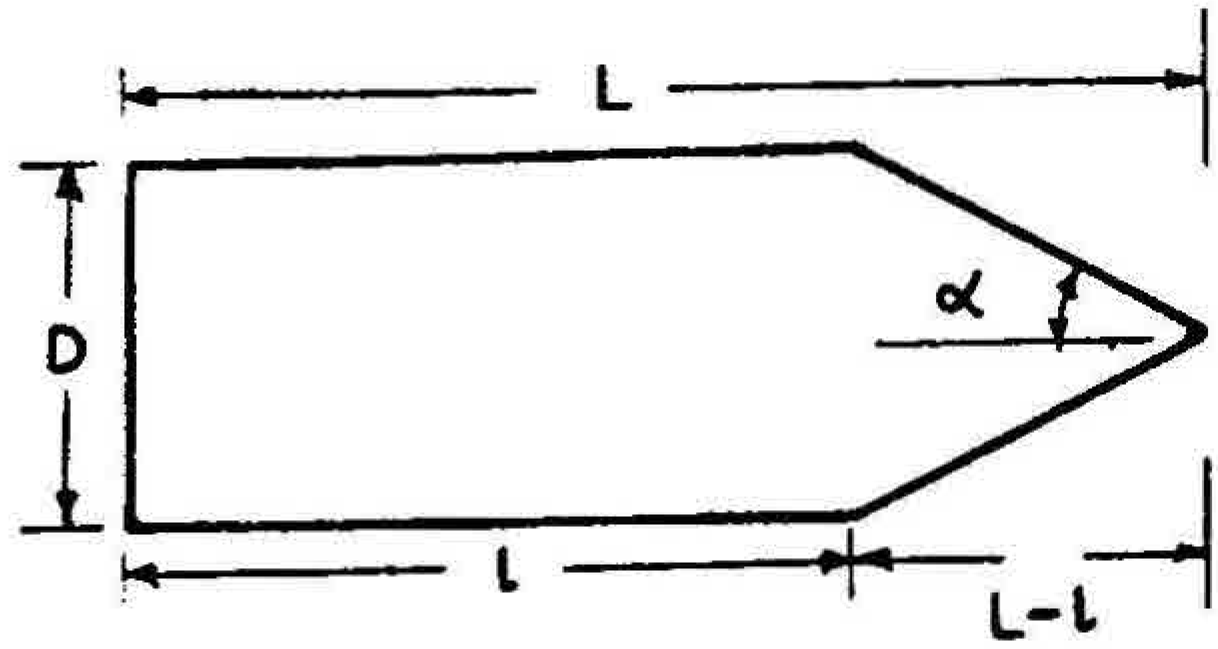

FIG. 2. Dimensional sketch of the wooden termination.

TABLE I

v.s.w.r. with Different Wooden Terminations

Wooden termination	Total length L in inches	Length of taper L−l in inches	Angle of taper degrees α	Diameter of the un-tapered end D inches	Maximum v.s.w.r.	Minimum v.s.w.r.
A	6	$2\frac{3}{4}$	9·7	$\frac{15}{16}$	1·15	1·09
B	6	$2\frac{9}{16}$	12·8	$1\frac{1}{4}$	1·17	1·02
C	6	$2\frac{11}{16}$	16·1	$1\frac{9}{16}$	1·15	1·08
D	6	$2\frac{13}{16}$	19·4	$1\frac{7}{8}$	1·20	1·08
E	6	$2\frac{9}{16}$	28·9	$2\frac{3}{16}$	1·10	1·02
F	6	$2\frac{1}{2}$	29·1	$2\frac{1}{2}$	1·12	1·02
G	$4\frac{1}{2}$	$2\frac{7}{8}$	14·4	$1\frac{3}{16}$	$>1·20$	$\cong 1·00$
H	$6\frac{1}{8}$	$2\frac{9}{16}$	30	$2\frac{3}{4}$	$>1·20$	$\cong 1·00$

respectively. The results reported in the above table and graphs were obtained with the probe in the E_z position.

(*ii*) *Absorbing Materials.*—Different absorbing materials such as glass-wool, sawdust, glass-wool with graphite powder sucked inside, etc., were attempted and the results are presented in Table II. Some of the results are presented graphically in Fig. 7 and Fig. 8. The materials designated by L, M, N, O are as follows:

L = Pencil graphite lining with termination 'H' at the receiving horn.

M = Carbon soot lining at the receiving horn.

N = Tracing paper lining at the receiving and the transmitting horn.

O = Pencil graphite lining at the receiving horn with a graphite coated card-board ring fixed outside the receiving horn.

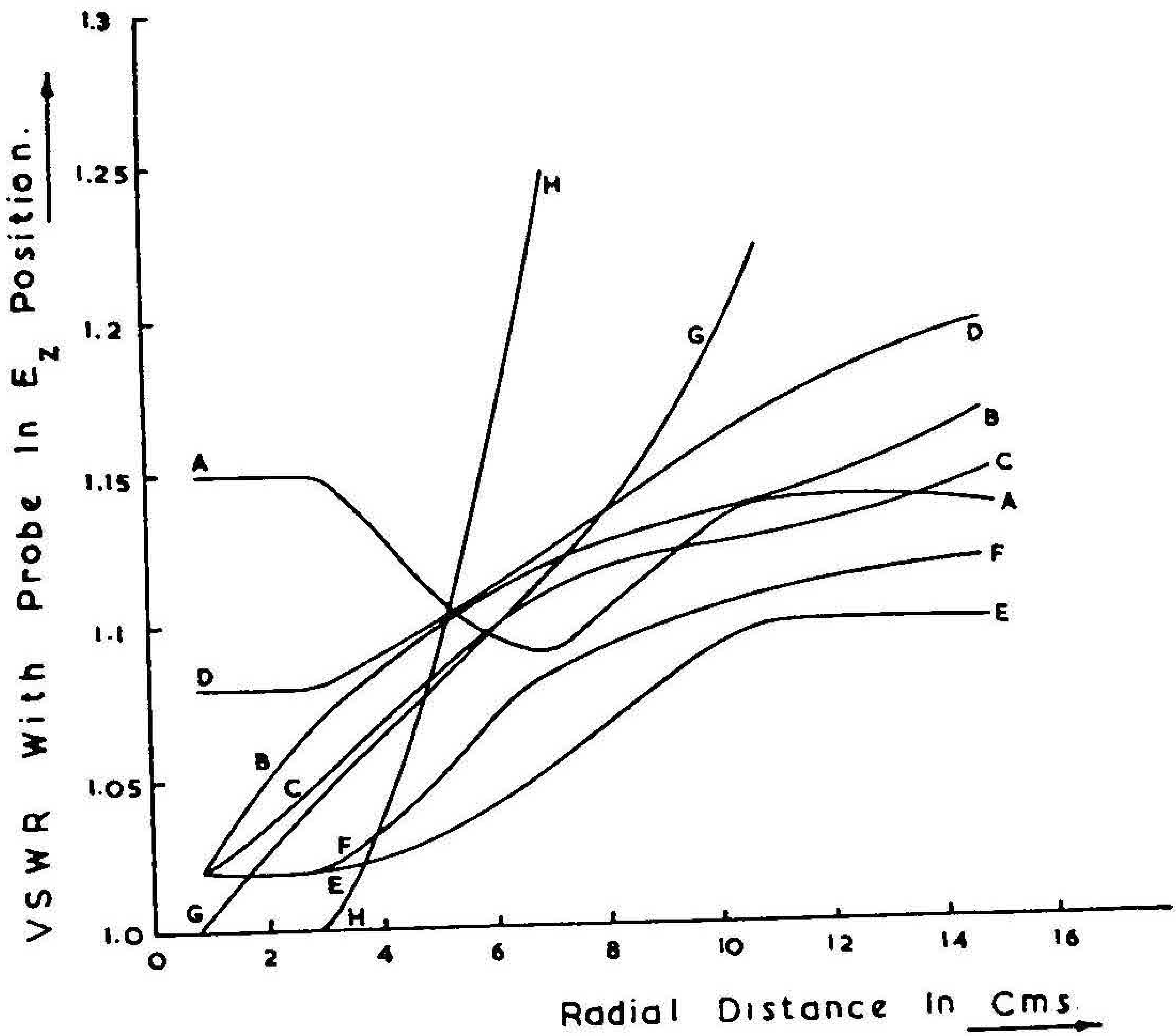

FIG. 3. Variation of v.s.w.r. with radial distance for wooden termination.

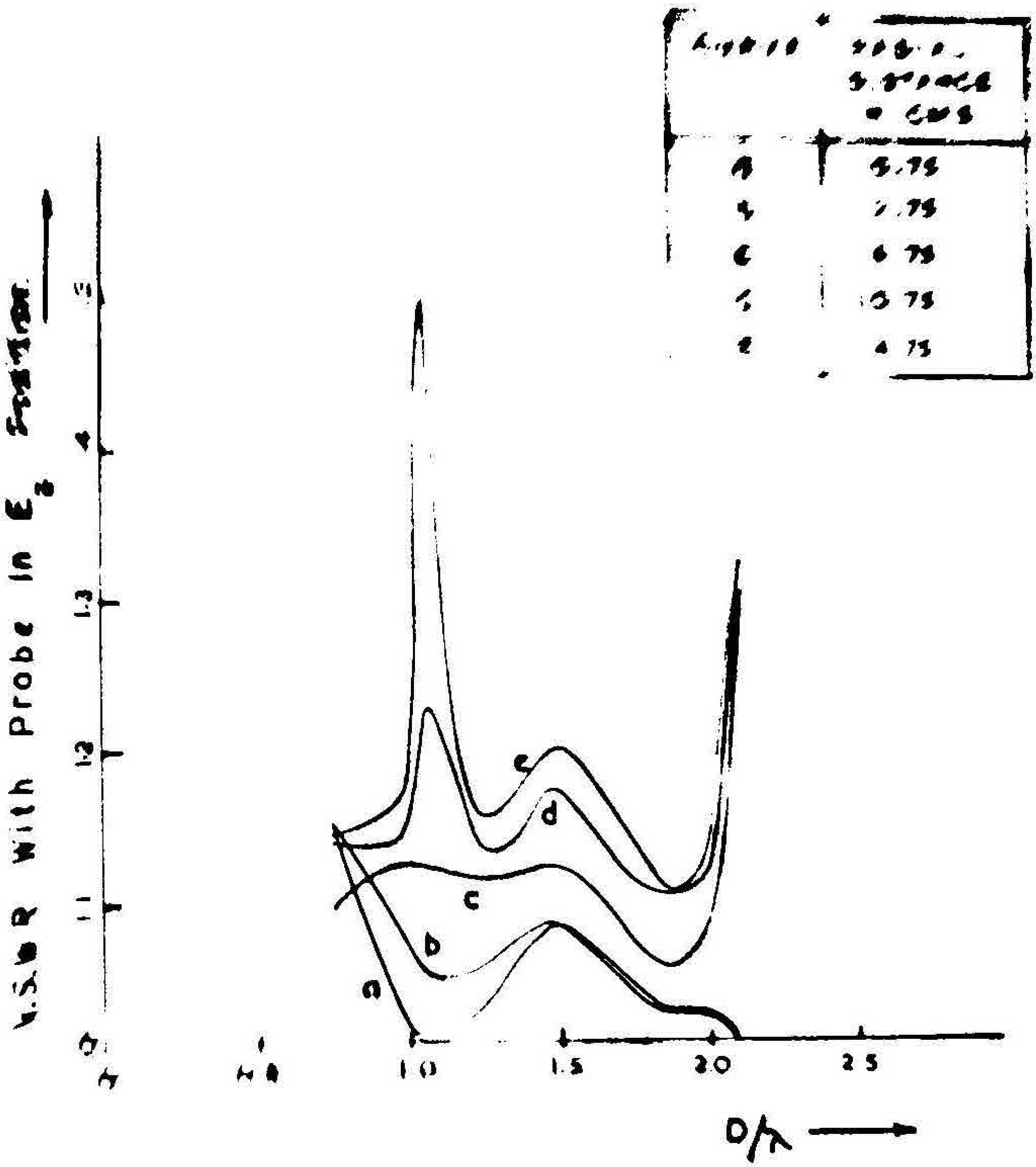

Fig. 1 Variation of V.S.W.R. with D/λ for wooden termination.

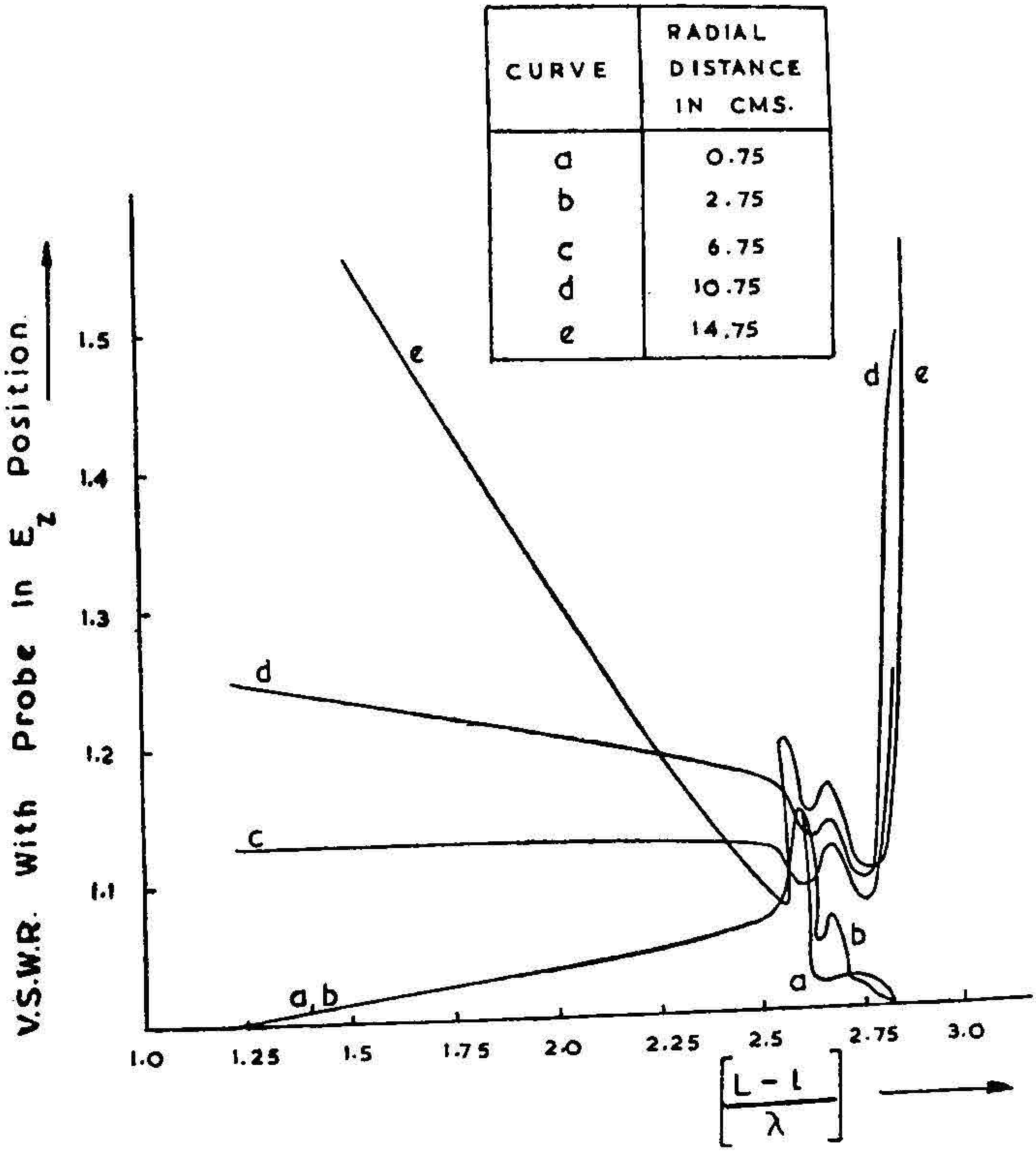

FIG. 5. Variation of v.s.w.r. with $(L-l)/\lambda$ for wooden termination.

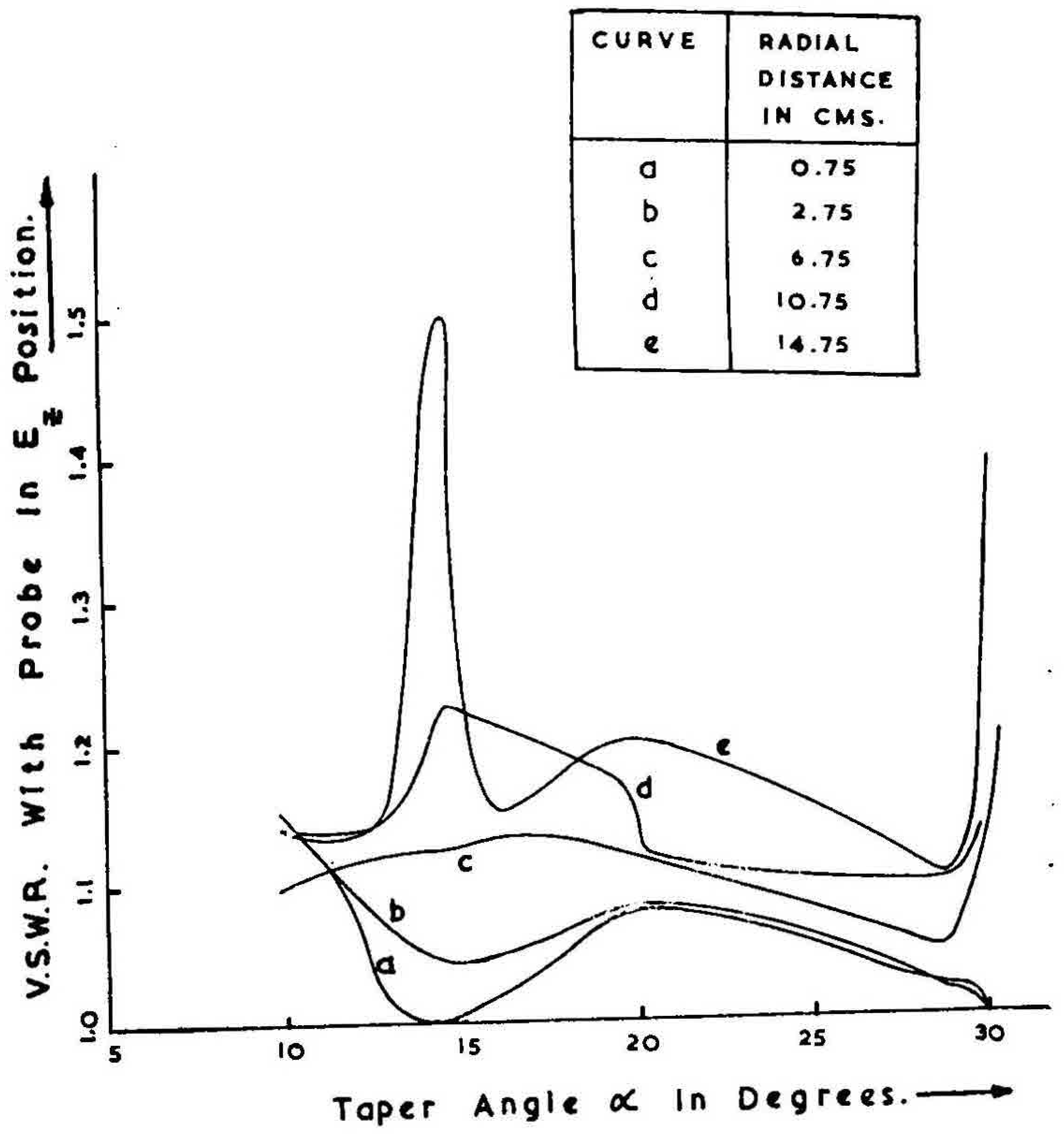

FIG. 6. Variation of v.s.w.r. with α for wooden termination

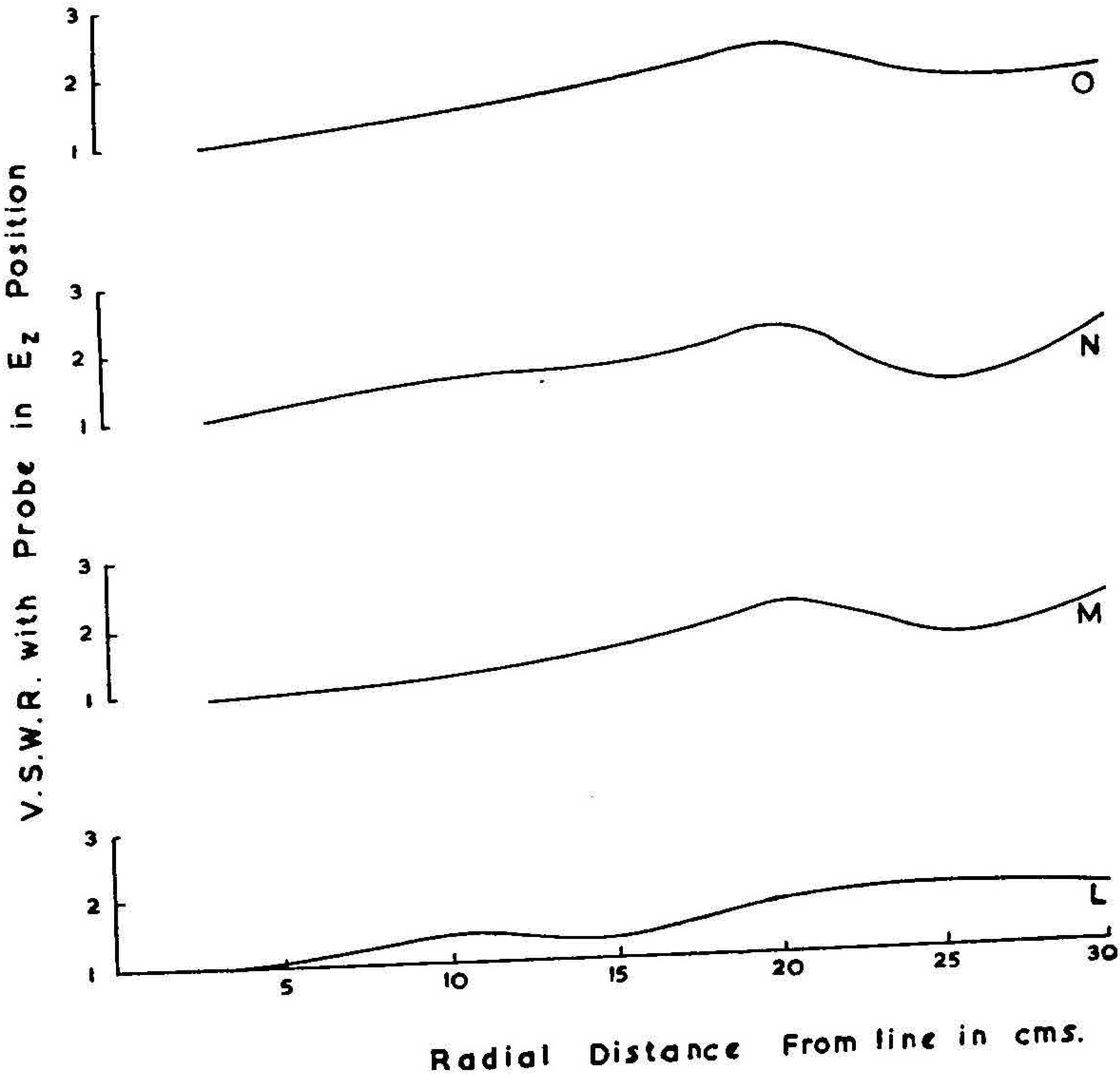

FIG. 7. Variation of v.s.w.r. with radial distance. Probe is placed in the E_z orientation. Termination is absorbing materials L, M, N, O.

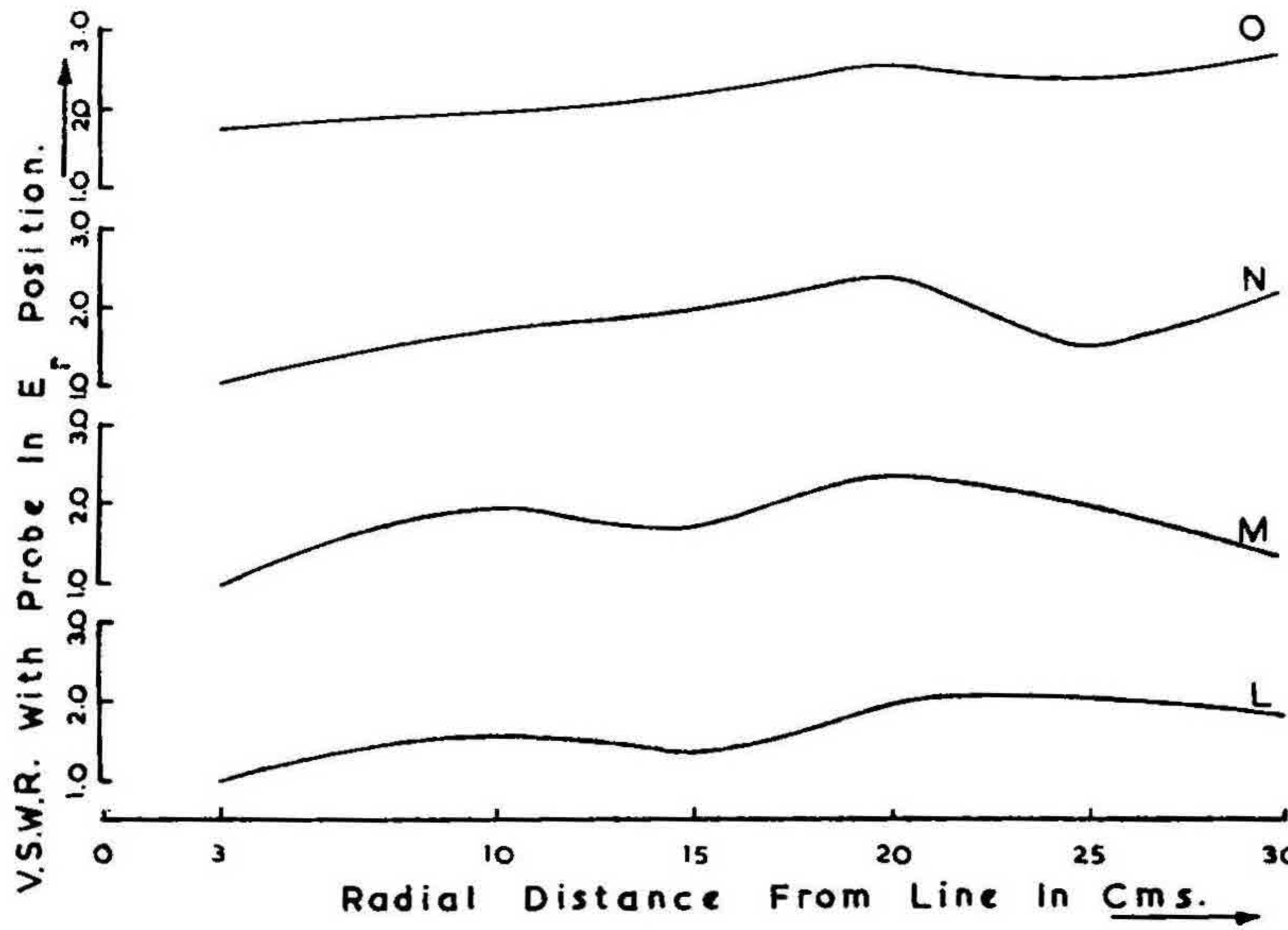

FIG. 8. Variation of v.s.w.r. with radial distance. Probe is placed in the E_r orientation. Termination is absorbing materials L, M, N, O.

It is to be noted that the packing of the material and the mixture were fixed arbitrarily.

TABLE II

v.s.w.r. with Different Absorbing Materials as Termination

Absorbing materials placed at the receiving horn	Radial distance from the line in cm.	Probe in E_z position		Probe in E_r position	
		Maximum v.s.w.r.	Minimum v.s.w.r.	Maximum v.s.w.r.	Minimum v.s.w.r.
Tracing paper lining in the receiving horn	3	≃1·00	≃1·00	1·00	≃1·00
	10	1·76	1·76	2·00	2·00
	15	2·23	2·23	2·45	2·45
	20	2·71	2·71	2·64	2·60
	25	1·46	1·41	1·43	1·40
	30	2·24	1·84	2·45	2·45
Tracing paper lining in the receiving horn packed with cotton	3	≃1·00	≃1·00	≃1·00	≃1·00
	10	2·00	1·87	≃1·00	≃1·00
	15	2·74	2·64	2·92	2·90
	20	2·91	2·91	2·00	1·98
	25	1·65	1·61	2·00	2·00
	30	2·58	2·45	3·00	2·90

TABLE II (*Contd.*)

Absorbing materials placed at the receiving horn	Radial distance from the line in cm.	Probe in E_z position		Probe in E_r position	
		Maximum v.s.w.r.	Minimum v.s.w.r.	Maximum v.s.w.r.	Minimum v.s.w.r.
Tracing paper lining in the receiving horn packed with absorbent cotton	3	$\simeq$1·00	$\simeq$1·00	1·73	1·72
	10	1·41	1·40	2·00	1·90
	15	1·50	1·50	2·24	2·24
	20	2·00	2·00	2·64	2·64
	25	1·58	1·58	2·45	2·45
	30	2·40	2·40	2·83	2·83
Tracing paper lining in the receiving horn packed with sawdust	3	$\simeq$1·00	$\simeq$1·00	1·21	1·20
	10	1·48	1·48	2·00	2·00
	15	1·29	1·25	1·33	1·30
	20	1·83	1·80	2·00	2·00
	25	1·66	1·66	1·58	1·58
	30	2·20	2·20	2·45	2·45
Tracing paper lining in the receiving horn packed with glass-wool	3	$\simeq$1·00	$\simeq$1·00	$\simeq$1·00	$\simeq$1·00
	10	1·40	1·32	1·20	1·20
	15	2·00	2·00	1·90	1·90
	20	2·30	2·25	2·20	2·20
	25	3·16	3·16	4·50	4·40
	30	>6·00	>6·00	>7·00	>7·00
Pencil graphite lining at the receiving horn	3	1·05	1·05	1·10	1·10
	10	1·82	1·80	2·24	2·20
	15	2·20	2·00	2·45	2·45
	20	1·58	1·58	1·82	1·82
	25	1·41	1·41	1·55	1·50
	30	1·68	1·68	1·73	1·73
50% pure graphite lining in the receiving horn	3	1·06	1·06	1·10	1·10
	10	1·61	1·61	1·80	1·80
	15	2·64	2·64	2·83	2·80
	20	1·74	1·74	1·87	1·87
	25	1·28	1·28	2·00	2·00
	30	1·41	1·40	1·50	1·50
Absorbing materials placed at both the receiving and the transmitting ends					
Both transmitting and receiving horn packed with glass-wool	3	1·05	1·05	$\simeq$1·00	$\simeq$1·00
	10	1·73	1·73	1·70	1·70
	15	2·00	1·58	1·60	1·58
	20	3·00	3·00	2·91	2·90
	25	3·46	3·46	3·10	3·10
	30	4·90	4·90	4·60	4·60

TABLE II (*Contd.*)

Absorbing materials placed at the receiving horn	Radial distance from the line in cm.	Probe in E_s position		Probe in E_r position	
		Maximum v.s.w.r,	Minimum v.s.w.r.	Maximum v.s.w.r.	Minimum v.s.w.r.
Both transmitting and receiving horn packed with sawdust	3	1·46	1·46	1·42	1·42
	10	1·84	1·84	1·50	1·50
	15	1·79	1·73	1·71	1·69
	20	1·73	1·73	1·66	1·65
	25	1·82	1·73	1·70	1·70
	30	1·41	1·29	1·30	1·30
Both transmitting and receiving horn packed with absorbent cotton	3	$\simeq$1·00	$\simeq$1·00	$\simeq$1·00	$\simeq$1·00
	10	1·41	1·41	1·40	1·38
	15	1·41	1·33	1·41	1·41
	20	1·85	1·85	1·67	1·67
	25	2·16	2·16	1·90	1·90
	20	2·24	2·24	1·99	1·99

(*iii*) *Wooden Termination with Fins.*—A dimensional sketch of the wooden termination with cardboard fins coated with graphite (Barlow *et al.*, 1953) is shown in Fig. 9. A photograph showing the position and orientation of the termination with respect to the receiving horn is shown in Fig. 10. The results of measurement for both the orientations of the probe are shown in Table III.

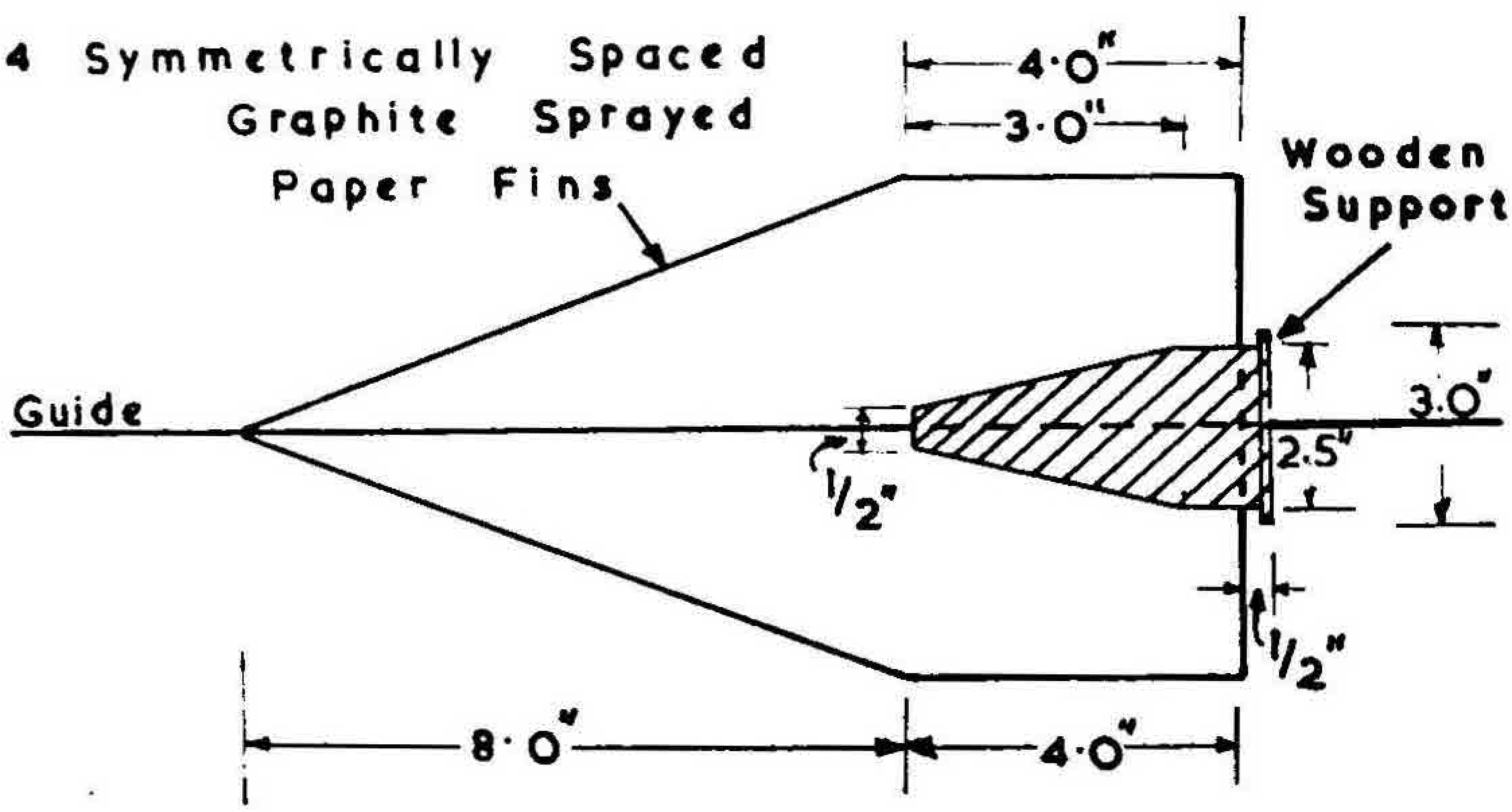

FIG. 9. Dimensional sketch of the wooden termination with fins. The cardboard fins are coated with graphite.

Some of the results are plotted graphically in Fig. 11 for the sake of comparison with other terminations.

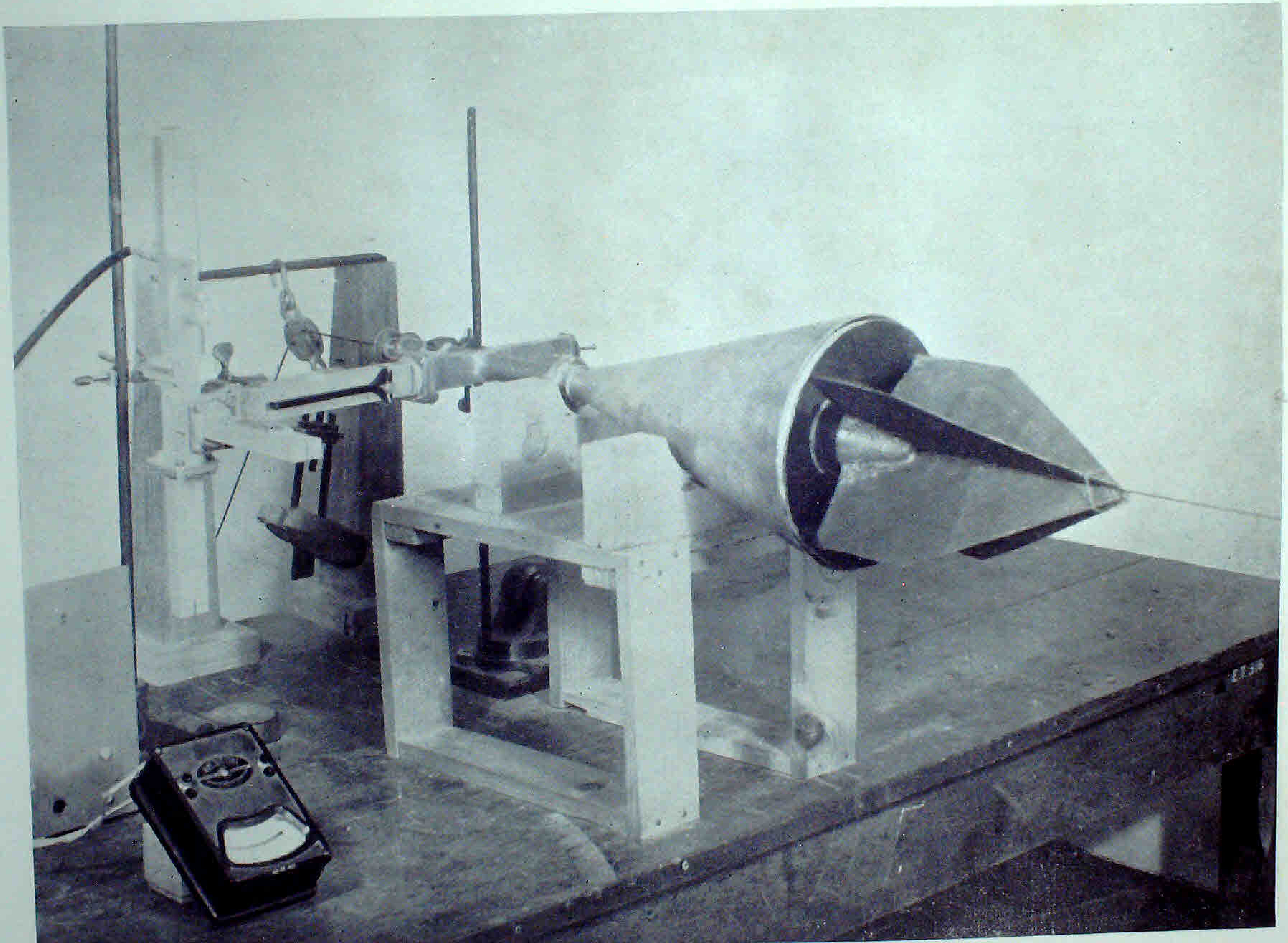

FIG. 10. Photograph showing the position and orientation of the wooden termination with fins coated with graphite.

TABLE III

v.s.w.r. with Wooden Termination with Fins

Radial distance from the surface of the line in cm.	Probe in the E_z position		Probe in the E_r position	
	Maximun v.s.w.r.	Minimum v.s.w.r.	Maximum v.s.w.r.	Minimum v.s.w.r.
3	$\simeq 1\cdot00$	$\simeq 1\cdot00$	$\simeq 1\cdot00$	$\simeq 1\cdot00$
10	$\simeq 1\cdot00$	$\simeq 1\cdot00$	$\simeq 1\cdot00$	$\simeq 1\cdot00$
15	$\simeq 1\cdot00$	$\simeq 1\cdot00$	$\simeq 1\cdot00$	$\simeq 1\cdot00$
20	$\simeq 1\cdot00$	$\simeq 1\cdot00$	$\simeq 1\cdot04$	$\simeq 1\cdot04$
25	$1\cdot02$	$1\cdot01$	$\simeq 1\cdot04$	$\simeq 1\cdot04$
30	$1\cdot04$	$1\cdot03$	$\simeq 1\cdot08$	$\simeq 1\cdot04$

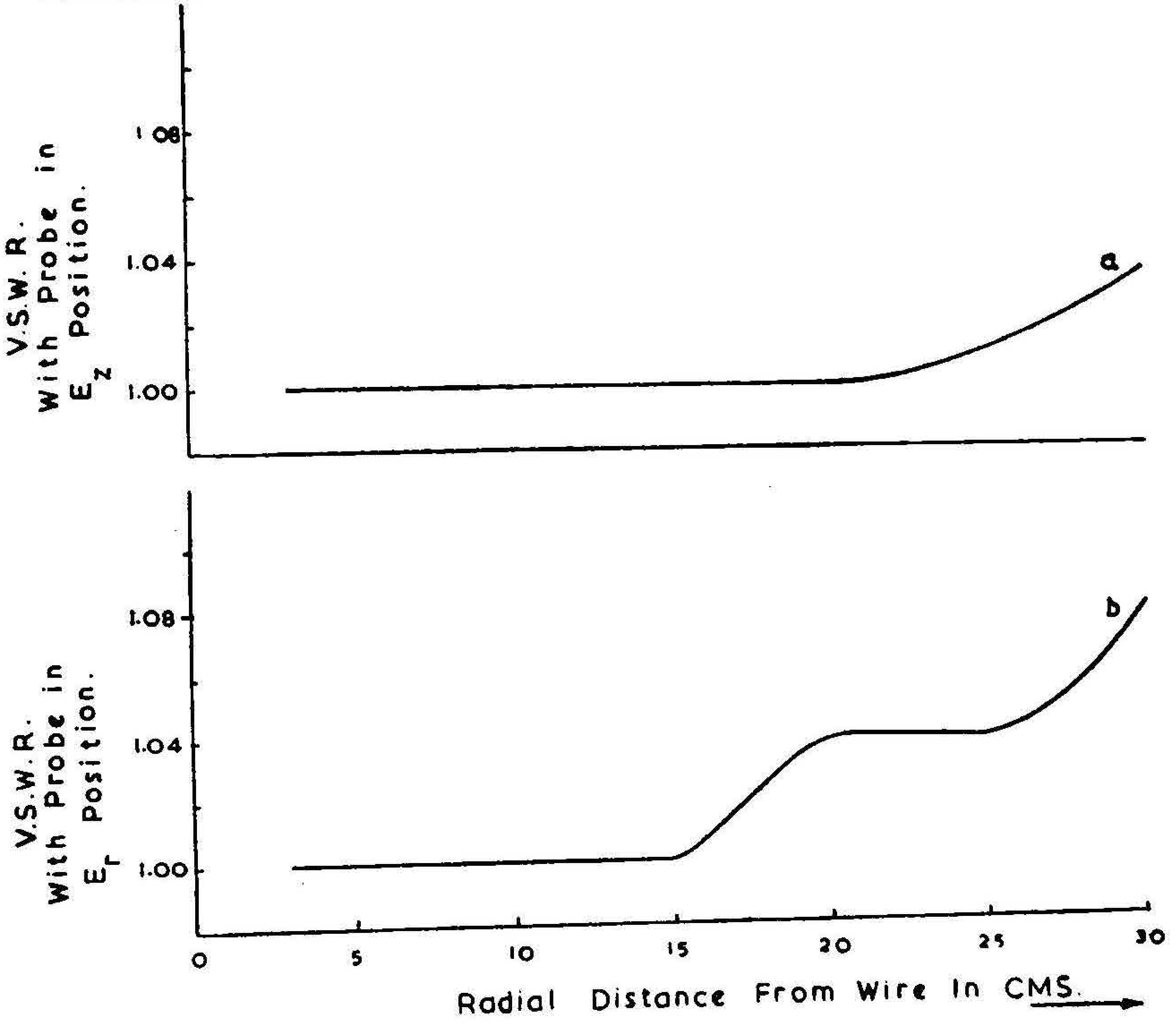

FIG. 11. Variation of v.s.w.r. with radial distance. Probe in the (*a*) E_z orientation; (*b*) E_r orientation. Termination is wooden with fins coated with graphite.

CONCLUSION

A comparative study of the results obtained with different terminations can be made from Table IV.

TABLE IV

A Comparative Study of the Matching with Different Terminations

Terminations	Radial distance in cm.	Difference between maximum and minimum v.s.w.r. with probe in the E_s position	Difference between maximum and minimum v.s.w.r. with probe in the E_r position
Wooden termination 'E' ..	2	0·08	
	6	0·06	
	10	0·01	
	14	0·01	
Absorbing Materials—			
Pencil graphite lining in the receiving horn	3	0	0
	10	0·42	0·58
	15	0·29	0·35
	20	0·82	1·00
	25	0·90	1·05
	30	0·87	0·82
Receiving horn packed with sawdust	3	0	0
	10	0·48	0·79
	15	0·29	0·12
	20	0·83	0·79
	25	0·66	0·37
	30	1·20	1·24
Wooden termination with fins	3	0	0
	10	0	0
	15	0	0
	20	0	0·04
	25	0·02	0·02
	30	0·04	0·08

It is observed from Table IV that the wooden termination with fins coated with graphite proves to be a better matching device than the other two. The reason may be due to the orientations of E_s, H_ϕ, and E_r with respect to the structure of the termination. Further work is under progress.

REFERENCES

Sommerfeld, A. ..	*Differential gleichungen der Physik*, 197, **2**, by Riemann-Weber, 1927, 507, 530.
Stratton, J. A. ..	*Electromagnetic Theory*, 1941, 527.
Chatterjee, S. K. and Madhavan, P.	*Jour. Ind. Inst. Sci.*, 1955, **37**, 200.
Barlow, H. M. and Karbowiak, A. E.	*Proc. I.E.E.*, Part III, 1953, **100**, 321.